THE JOURNAL OF BIOLOGICAL CHEMISTRY VOL. 289, NO. 26, pp. 18122–18136, June 27, 2014

Disulfide Bond Requirements for Active Wnt Ligands*

Received for publication, April 19, 2014, and in revised form, May 16, 2014 Published, JBC Papers in Press, May 19, 2014, DOI 10.1074/jbc.M114.575027

Bryan T. MacDonald[‡1], Annie Hien[‡1], Xinjun Zhang[‡], Oladoyin Iranloye[‡2], David M. Virshup[§], Marian L. Waterman[¶], and Xi He[‡3]

From the [‡]F. M. Kirby Neurobiology Center, Boston Children's Hospital, Department of Neurology, Harvard Medical School, Boston, Massachusetts 02115, the [§]Program in Cancer and Stem Cell Biology, Duke-National University of Singapore Graduate Medical School, 8 College Road, 169857 Singapore, and the [¶]Department of Microbiology and Molecular Genetics, University of California, Irvine, California 92697

Background: Wnt proteins are rich in cysteines, but their functional significance has not been systematically examined.
Results: Mutagenesis of cysteines in Wnt3a uncovers their requirements for Wnt secretion and/or receptor binding.
Conclusion: Behaviors of the Wnt3a cysteine mutants are consistent with the Wnt structure model.
Significance: This study provides insights into pathogenesis associated with WNT mutations and new tool sets for WNT research.

Secreted Wnt lipoproteins are cysteine-rich and lipid-modified morphogens that bind to the Frizzled (FZD) receptor and LDL receptor-related protein 6 (LRP6). Wnt engages FZD through protruding thumb and index finger domains, which are each assembled from paired *β* strands secured by disulfide bonds and grasp two sides of the FZD ectodomain. The importance of Wnt disulfide bonds has been assumed but uncharacterized. We systematically analyzed cysteines and associated disulfide bonds in the prototypic Wnt3a. Our data show that mutation of any individual cysteine of Wnt3a results in covalent Wnt oligomers through ectopic intermolecular disulfide bond formation and diminishes/abolishes Wnt signaling. Although individual cysteine mutations in the amino part of the saposin-like domain and in the base of the index finger are better tolerated and permit residual Wnt3a secretion/activity, those in the amino terminus, the thumb, and at the tip of the index finger are incompatible with secretion and/or activity. A few select double cysteine mutants based on the disulfide bond pattern restore Wnt secretion/activity. Further, a double cysteine mutation at the index finger tip results in a Wnt3a with normal secretion but minimal FZD binding and dominant negative properties. Our results experimentally validate predictions from the Wnt crystal structure and highlight critical but different roles of the saposin-like and cytokine-like domains, including the thumb and the index finger in Wnt folding/secretion and FZD binding. Finally, we modified existing expression vectors for 19 epitope-tagged human WNT proteins by removal of a tag-supplied ectopic cysteine, thereby generating tagged WNT ligands active in canonical and non-canonical signaling.

Secreted Wnt proteins have essential roles in embryogenesis, homeostasis, and pathogenesis though activation of canonical/*β*-catenin and non-canonical (*β*-catenin-independent) pathways (1–3). Wnt proteins are ~350 amino acids in size and cysteine-rich and undergo several post-translational modifications during biogenesis, including the addition of a palmitoleic acid moiety, multiple *N*-glycosylations, and the coordination of a series of disulfide bonds (4, 5). The human genome encodes 19 WNT proteins, which can be divided into 12 paralogous groups (6) and have been shown to signal through a multitude of seven-transmembrane Frizzled receptors (FZD1 to -10) and single-transmembrane Wnt receptors or coreceptors, including LRP5/6, ROR1/2, RYK, and others (7, 8). It is generally thought that the receptor complex dictates the signaling pathway choice initiated by the Wnt ligand, as best illustrated in the case of FZD and LRP5/6 for *β*-catenin signaling (1).

The most studied mammalian Wnt is mouse Wnt3a. Cells stably transfected with Wnt3a cDNA readily secrete detectable levels of functional Wnt3a protein, which can be collected as conditioned medium (CM)[4] and applied to cells to activate *β*-catenin and non-canonical signaling (9). These qualities have facilitated the purification of recombinant Wnt3a in its active glycosylated/lipidated form and made Wnt3a the *de facto* prototypic Wnt (10). Wnt3a has two predicted *N*-glycosylation sites (N*X*(S/T)) at Asn-87 and Asn-287, which have been validated experimentally and shown to be required for Wnt secretion (11). Importantly Wnt3a is recognized to be lipidated (10) with a palmitoleic acid moiety at Ser-209 (12), a modification that is required for Wnt3a secretion and appears to be carried out by Porcupine (*PORCN*), a member of the membrane-bound *O*-acyltransferase family (13–15). Indeed, the Wnt3a S209A mutant is not secreted and is unable to bind to Wntless (*WLS*, also known as *GPR177*, *Evi*, or *Sprinter*) (12, 16), a multitransmembrane chaperone that serves as dedicated trafficking machinery for lipidated Wnt ligands. The lipid modification and involvement of PORCN and WLS appear to be universal for biogenesis of all vertebrate/mammalian Wnt proteins (4).

* This work was supported, in whole or in part, by National Institutes of Health Grants RO1 GM074241 and RO1 AR060359 (to X. H.).
[1] Both authors contributed equally to this work.
[2] A Harvard SHURP (Summer Honors Undergraduate Research Program) intern.
[3] Holder of an endowed research chair of Boston Children's Hospital (BCH) and supported by BCH Intellectual and Developmental Disabilities Research Center Grant P30 HD-18655. To whom correspondence should be addressed. Tel.: 617-919-2257; Fax: 617-919-2771; E-mail: xi.he@childrens.harvard.edu.

[4] The abbreviations used are: CM, conditioned medium; CRD, cysteine-rich domain; STF, SuperTopFlash.

Another striking feature of Wnt proteins is their conserved 24 (such as Wnt3a) or 22 (such as Wnt8) cysteine residues spread across the entire length of the molecule. Cys-77 of Wnt3a has been studied extensively because it was initially considered a lipidation site (10). The Wnt3a C77A mutant, in contrast to the S209A mutant, is secreted normally but displays diminished activity (10–12, 17). In Triton X-114 detergent-aqueous phase separation assays, Wnt3a is hydrophobic and partitions in the detergent phase, a characteristic of lipid adduction, but the C77A mutant is hydrophilic and partitions in the aqueous phase (10–12). However the crystal structure of *Xenopus* Wnt8 (Xwnt8) shows that the equivalent cysteine is involved in disulfide bonding and is not lipid-modified (18). Consistent with this finding, our study shows that Wnt3a C77A is lipidated normally but forms ectopic intermolecular disulfide bonds and thus large oxidized aggregates, which exhibit hydrophilic partitioning, possibly via burying the Ser-209 palmitoleic acid moiety within the oligomerized C77A mutant (19). This aggregate behavior probably accounts for the poor ability of Wnt3a C77A to bind to FZD or LRP6 extracellular domains (11, 17). Thus, the integrity of disulfide bonds of a Wnt protein appears to be critical for its structure and function.

The crystal structure of Xwnt8 in complex with FZD8 CRD, the extracellular cysteine-rich domain (CRD) of FZD8, represents the first and only known complete Wnt protein structure, revealing a glycosylated Wnt8 with a single lipid adduct at Ser-187 (the equivalent of Ser-209 of Wnt3a) plus 11 disulfide bonds formed among 22 cysteines (18). The Wnt8 structure resembles a hand with a large palm region and two finger-like protrusions (referred to as the "thumb" and "index finger," respectively), which consists of looping β strands that are stabilized by several disulfide bonds, and act to pinch together in opposition to bind FZD8 CRD (Fig. 1*A*). The Wnt8 thumb points the lipid adduct outward to insert between two hydrophobic helices in FZD8 CRD (site 1), and the Wnt8 index finger ends in a vicinal disulfide bond that wraps around the other edge of the CRD (site 2) (18). A crystallized interface between a Wnt ligand and the LRP6 co-receptor is yet to be reported; however, a constellation of conserved residues in the Wnt palm region probably contribute to LRP6 binding (18, 20). Indeed a series of positively charged residues in the Wnt3a palm region were recently shown to be important for LRP6 interaction (21).

Bioinformatic and structural analyses have suggested a hypothesis that Wnt proteins evolved from an ancient fusion of two polypeptides, a saposin-like domain (D1) and a cytokine-like domain (D2), to impart bivalent binding to FZD (20). However, the significance of these Wnt domains and the many disulfide bonds that bolster their structures has not been experimentally examined. Here we systematically mutated each cysteine individually and in selected pairwise combinations in Wnt3a and characterized their effect on Wnt3a secretion and signaling activity. In addition, we constructed and examined a modified version of expression vectors for 19 human WNT proteins that are carboxyl-terminally tagged and appear to be functional in canonical and/or non-canonical Wnt signaling, thereby facilitating future characterization of all WNT proteins.

EXPERIMENTAL PROCEDURES

Plasmids—Mouse *Wnt3a* cDNA (from the LNCX-Wnt3a vector and containing 104 bp of 5′-UTR and 270 of 3′-UTR) was subcloned into the pCS2 expression vector using the EcoRI site. Cysteine to alanine amino acid substitutions were generated using the QuikChange mutagenesis kit (Stratagene). Untagged and V5-tagged human WNTs in pcDNA3.2/V5-DEST vector were described previously in the Open Source *WNT* Project (22). Additional carboxyl-terminal amino acids added in the published V5-tagged WNT constructs, referred to here as "(+C linker)," +CILKGGRADPAFLYVVDLLGPRFEGKPIPNPLLGLDSTRTG (V5 tag is underlined), were altered to +GGGKPIPNPLLGLDSTRTG using the QuikChange mutagenesis strategy with the inclusion of 0.1% DMSO to relieve secondary structure in the deletion/replacement region. Sequence information on mutagenesis primers is available upon request.

Dual Luciferase Assay—Mammalian cell transfections were performed in HEK293T (ATCC CRL-11268) cells using FuGENE 6. Cells were plated at 0.5×10^5/ml in 24-well plates and transfected the following day with a total of 200 ng of DNA/well (50 ng of SuperTopFlash (STF)- or TOPFLASH Wnt-responsive reporter plasmid, 5 or 10 ng of control thymidine kinase promoter *Renilla*, and up to 50 ng of experimental DNA constructs. The total amount of transfected DNA is balanced with the pCS2+ empty vector. To increase canonical β-catenin signaling, 1 ng of VSVG-LRP6 was included as described previously (23). For CM activity experiments, CM was collected from 6-well plates transfected with 500 ng of Wnt3a constructs 40–48 h post-transfection and applied to 24-well plates transfected with 50 ng of TOPFLASH, 10 ng of thymidine kinase promoter *Renilla*, and 40 ng of $pCS2^+$ (empty vector). The lysates were collected 40–48 h post-transfection and used with the Dual-Luciferase reporter system (Promega), assayed as described previously (24). Normalized data expressed in relative luciferase units was averaged from triplicate assays, and the *error bars* reflect the S.D. values. Representative data are presented from one of at least three independent experiments.

Immunoblotting and Antibodies—Western blots were performed as described previously (24). For non-reducing conditions, 2% β-mercaptoethanol was omitted from the protein loading buffer. The following commercially available antibodies were used: Wnt3a (C64F2, Cell Signaling), DVL3 (4D3, Santa Cruz Biotechnology, Inc.), V5 (V8012, Sigma), or V5 (R960, Invitrogen). Wnt3a secretion was analyzed from HEK293T cells in 12-well plates transfected with 200 ng of Wnt3a expression constructs using Lipofectamine 2000. Relative density was measured using ImageJ to determine the amount of Wnt3a protein secreted into the medium under reducing conditions (normalized to lysate Wnt3a levels) and of monomeric Wnt3a protein measured under the non-reducing conditions (normalized to a 45 kDa nonspecific band). Data from multiple experiments was normalized to the WT Wnt3a amount (set at 100%), and the relative density with adjusted S.D. is reported in Table 1. For detection of Dishevelled phosphorylation, Rat2 cells were used because they exhibit low basal phosphorylation. Rat2 cells in 24-well plates were transfected with 100 ng of WNT in pcDNA3.2 using Lipofectamine LTX with

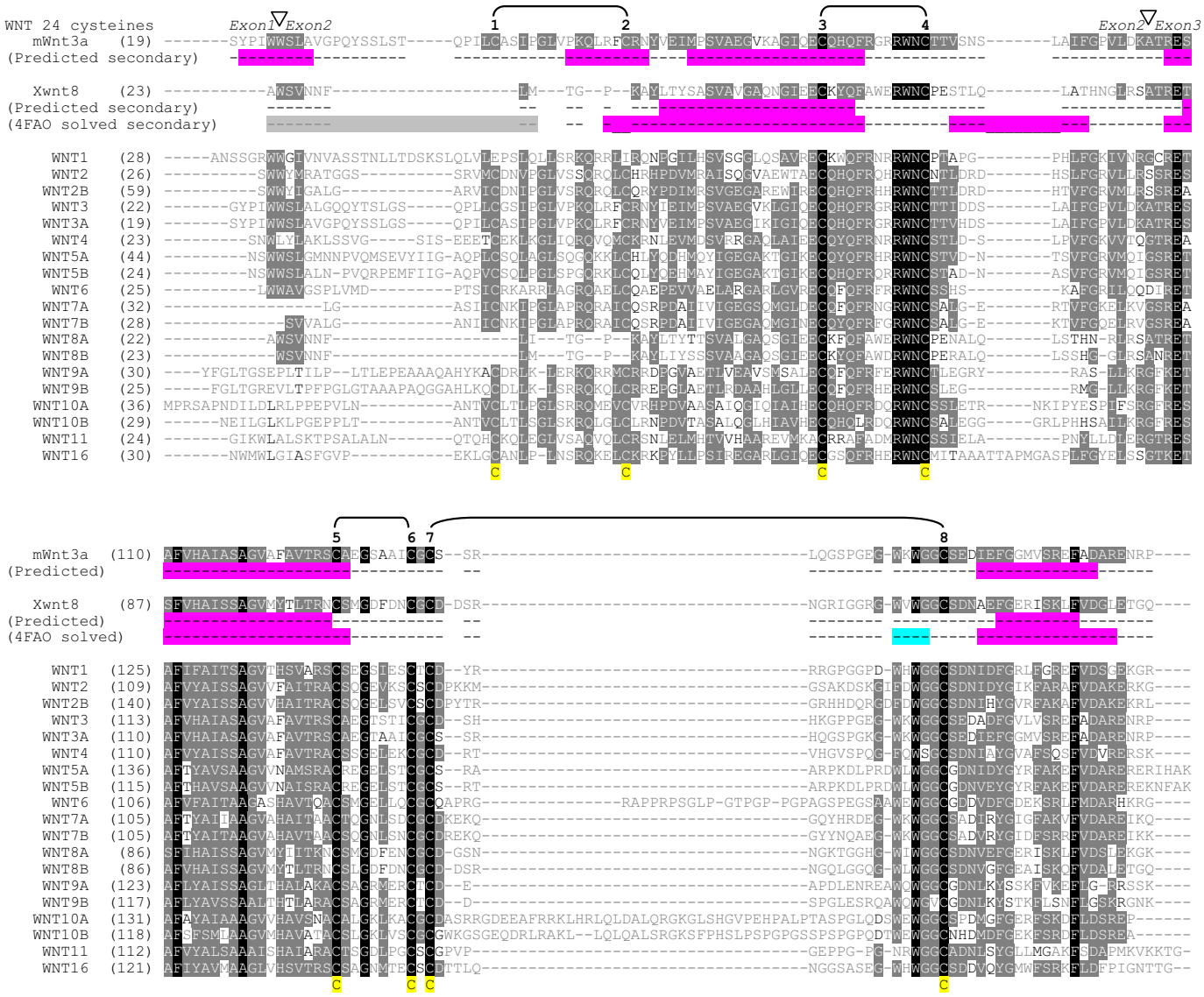

FIGURE 1. **Sequence alignment of mouse Wnt3a, *Xenopus* Wnt8, and all human WNT proteins using ClustalW.** Identical (*black background*, *white text*), conservative (*dark gray background*, *white text*), and similar (*light gray background*, *black text*) residues are highlighted. Wnt3a exon/intron boundaries are shown *above* the mature Wnt3a protein sequence. Cysteines 1–24 are *numbered* based on Wnt3a and highlighted in *yellow* below the alignment. *Green P* indicates palmitoleoylation site. The Wnt3a secondary structure shown *below* the Wnt3a sequence is predicted by PSIPRED. The Xwnt8 secondary structure predicted by PSIPRED and that resolved in the crystal structure (Protein Data Bank entry 4FOA) are shown *below* the Xwnt8 sequence, respectively: α helices (*magenta*), β sheets (*light blue*), and unresolved regions (*light gray*).

PLUS. Lysates were analyzed 20–24 h post-transfection on a 6% SDS-polyacrylamide gel to analyze phosphorylation mobility shift in Dishevelled proteins. FZD8 CRD IgG immunoprecipitation of Wnt3a was performed as described previously (19).

RESULTS

Wnt Subdomains and Analyses of Single Cysteine Mutants of Wnt3a—It has been suggested that Wnt proteins probably have evolved from the ancient fusion of a saposin-like (D1) and a cytokine-like (D2) domain to impart bivalent binding to the FZD CRD (20). For most *Wnt* genes, this putative fusion event is perhaps reflected in the last exon that encodes the D1 thumb/hairpin 2 and fourth helix of the saposin-like domain contiguous with the entire D2 cytokine-like domain (Fig. 1). Most *Wnt* genes, such as *Wnt3a*, are encoded by four exons, with the three additional exons encoding the signal peptide (the first exon), the signal peptide cleavage site and the amino-terminal region (the second exon), and saposin-like helices 1–3 and hairpin 1 (the third exon), respectively (Fig. 1). Based on the exon organization, cysteine disulfide pairings, and Xwnt8 crystal structure, we further subdivided the saposin-like domain into helical bundle-hairpin 1 and hairpin 2/thumb regions and subdivided the cytokine-like domain into cysteine knot and hairpin 3/index finger regions, in addition to the previously assigned amino-terminal region and the linker region between D1 and D2 (Fig. 2, *A* and *B*). Compared with most Wnts, Xwnt8 and human WNT8A/8B paralogues have a shorter amino region containing only two cysteines (Fig. 1) that form a disulfide bond and help to position the Xwnt8 first α helix perpendicular to the saposin-like helical bundle (18). Most Wnts, including Wnt3a,

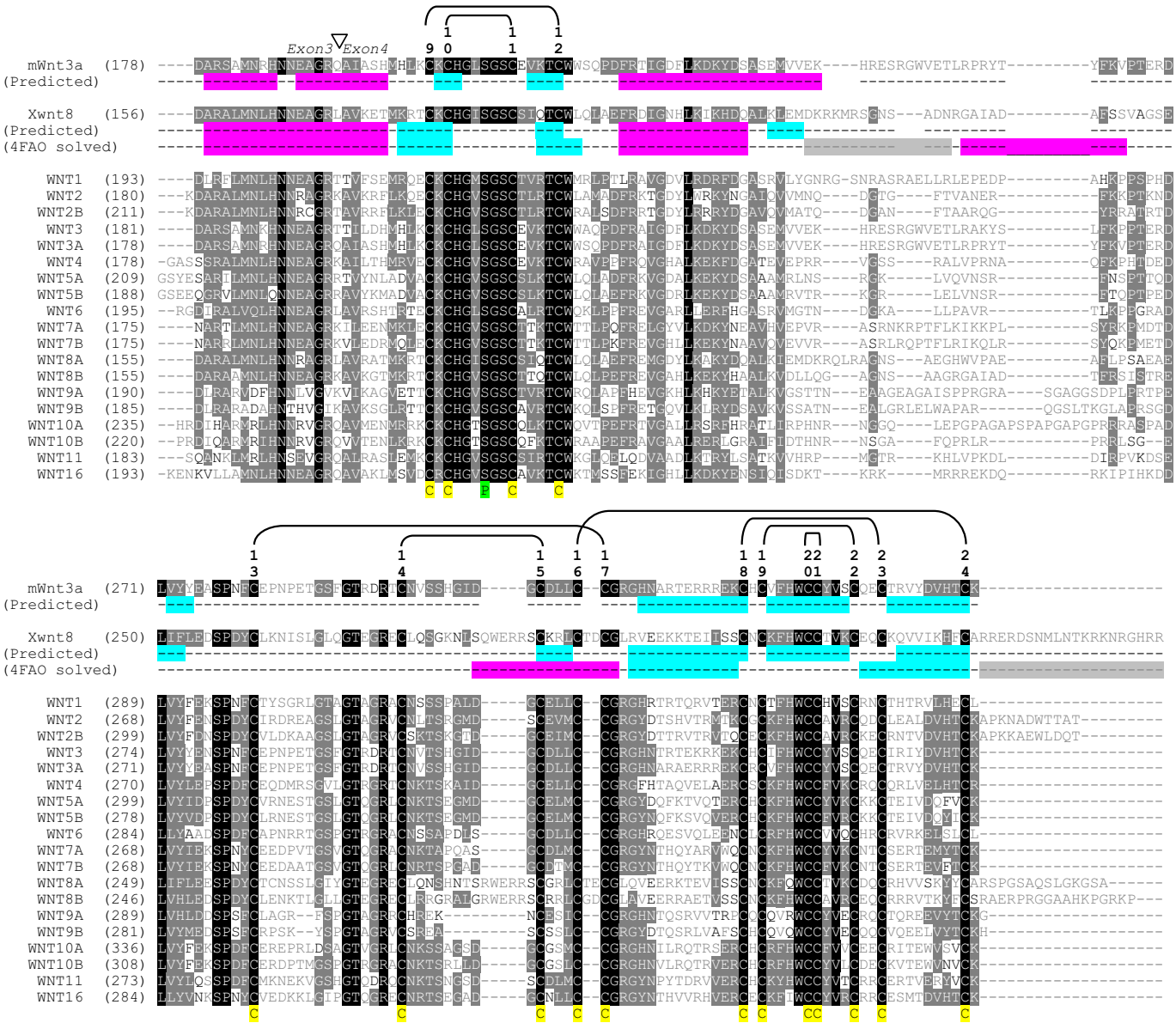

FIGURE 1—*continued*

contain a longer amino extension with two additional cysteines and one or more predicted α helices (Fig. 1). We have numbered the cysteines of Wnt3a, c1–c24, to reflect disulfide bonds based on the Xwnt8 structure (Fig. 2*B*). The 24 cysteines of Wnt3a are contained in the following Wnt subregions: amino (c1–4), hairpin 1 (c5–c8), hairpin 2/thumb (c9–c12), cysteine knot (c13–c17 and c24), and hairpin 3/index finger (c18–c23). The saposin-like helical bundle region and the linker region are noticeably devoid of cysteines (Fig. 2*B*).

To examine the importance of each disulfide bond, we engineered alanine substitution for each cysteine in a Wnt3a expression construct. The WT and mutant Wnt3a were each expressed in HEK293T cells, and protein levels were assessed in the cell lysate and CM using a Wnt3a antibody, which recognizes an epitope in the linker region. Wnt3a cysteine mutants were each detected in the cell lysate at levels comparable with that of the WT. CM was analyzed using a reducing buffer to analyze the Wnt3a secretion level (Fig. 2*C*). CM was also analyzed with non-reducing loading buffer lacking β-mercaptoethanol (Fig. 2*C*, *top gel*) in order to distinguish the monomeric Wnt3a and the high molecular weight Wnt3a oligomers, which are oxidized products of ectopic intermolecular disulfide bond formation among Wnt3a molecules (19).

Under the non-reducing condition, the WT Wnt3a is predominantly monomeric in CM. Consistent with our previous results, the Wnt3a c3 (C77A) mutant displayed secretion similar to WT when examined under reducing conditions but in fact predominantly formed high molecular weight oxidized oligomers that were obvious under the non-reducing condition (19). Based on the Xwnt8 structure, Wnt3a c3 and c4 probably form a disulfide bond (18). Wnt3a c4 mutation produced effects similar to those of the c3 mutation although with slightly more monomeric Wnt3a protein (Fig. 2*C*). In contrast, mutation at either c1 or c2 in the amino extension region greatly impaired

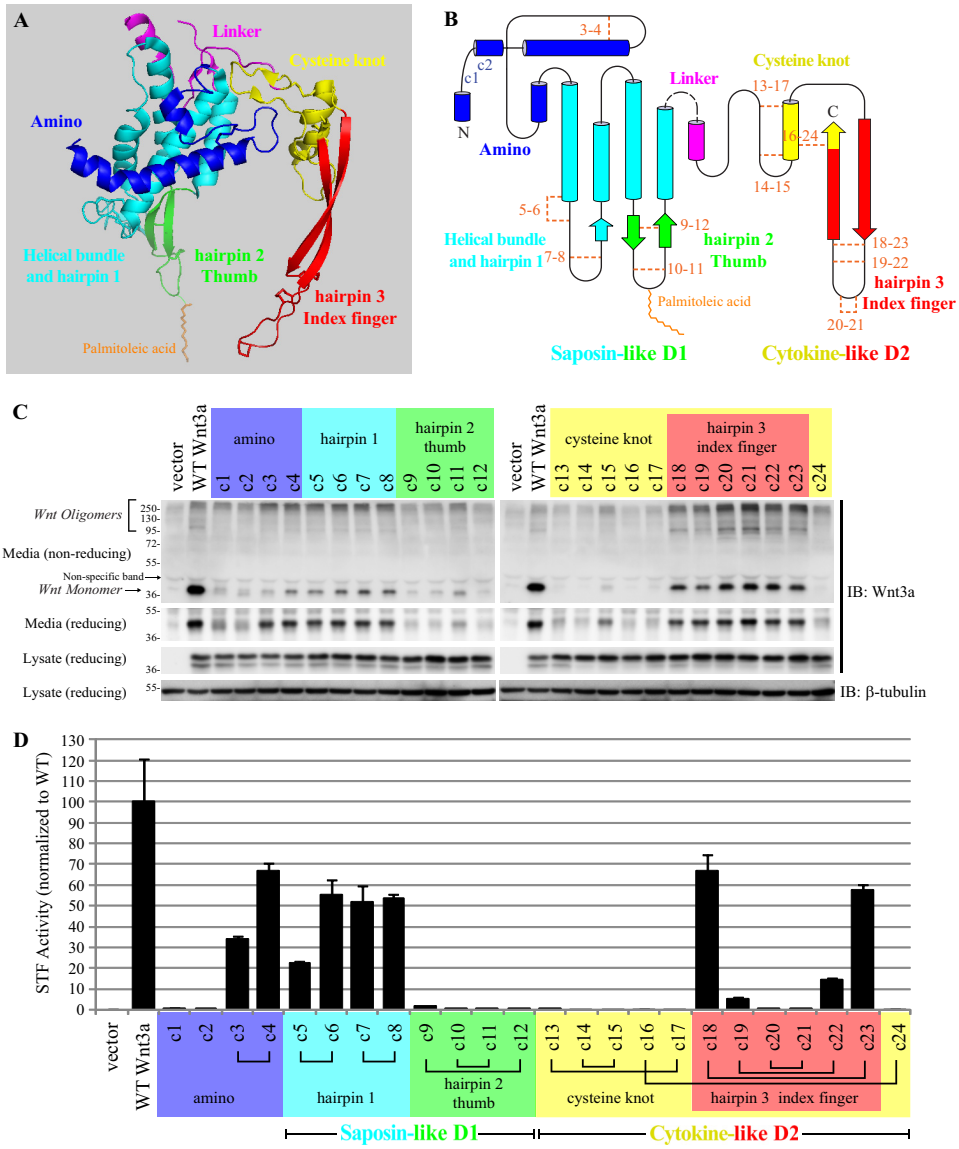

FIGURE 2. **Requirement of the individual 24 cysteines of Wnt3a for secretion and/or activity.** *A*, the structure and subdomains of Xwnt8 (Protein Data Bank entry 4FOA) with schematic α helices and β sheets. *B*, flat diagram showing the 24 cysteines of Wnt3a with the known ensemble of disulfide bonds modeled from the Xwnt8 structure. Note that Xwnt8 lacks the first two conserved cysteines (c1 and c2) found in the very amino-terminal region of most Wnt proteins. *C*, detection of protein levels of Wnt3a cysteine mutants in the whole cell lysate and in CM using an anti-Wnt3a antibody. Wnt3a in CM was further analyzed using reducing and non-reducing conditions to show the relative amounts of monomeric Wnt3a proteins. Relative density of the Wnt3a protein is quantified in Table 1. *D*, activity of the Wnt3a cysteine mutants determined by cotransfection with plasmids for Wnt-responsive STF luciferase and control *Renilla* luciferase reporters. Wnt3a was transfected at 10 ng/well in triplicate. Values were normalized to that of the WT Wnt3a set at 100%. *Error bars*, adjusted S.D. *IB*, immunoblot.

secretion (Fig. 2*C*). There is no structural analogy applicable for this portion of Wnt3a because Xwnt8 has neither c1 nor c2.

Unlike most saposin or saposin-like domains, which contain three disulfide bonds within the helical bundle (25), the Wnt c5–c6 and c7–c8 disulfide bonds are grouped in hairpin 1 between the first and second α helices of the saposin bundle, with hairpin 1 pointing toward the lipid-modified thumb/hairpin 2 (18, 20) (Fig. 2*B*). Secretion was not impaired for the four cysteine mutants in hairpin 1 (Fig. 2*C*). When examined under the non-reducing condition, however, these secreted mutants predominantly formed oxidized oligomers, with a minor monomeric fraction comparable with that of the c4 mutant (Fig. 2*C*).

Extending from the region between the saposin-like third and fourth helices, the thumb region features β sheets stabilized probably by two disulfide bonds, c9–c12 and c10–c11. Secretion was greatly impaired for the thumb cysteine mutants (Fig. 2*C*). Palmitoleoylation at the thumb tip by Porcupine (PORCN) and subsequent binding by Wntless (WLS) are essential for Wnt biogenesis and secretion. The thumb cysteine mutants thus bear a resemblance to the previously described S209A mutant, which is not secreted (12, 19). Mutation at each of the thumb cysteines probably destabilizes the region, potentially disrupting the interaction of Wnt3a with PORCN and/or WLS.

The cysteine knot region contains three disulfide bonds, c13–c17, c14–c15, and c16–c24, although only the c16–c24 disulfide bond is positioned similarly to that of cytokines (20). It is also noteworthy that c24 is the penultimate residue of most Wnt proteins (Fig. 1). Similar to the thumb cysteine mutants,

the cysteine mutation in this region rendered Wnt3a hardly detected in the CM; the exception was the c15 mutant, which showed some secretion but was mostly oxidized oligomers (Fig. 2*C*).

The index finger consists of two long β strands extending from the cysteine knot of the cytokine-like domain (Fig. 2, *A* and *B*). The index finger contains two disulfide pairs (c18-c23 and c19-c22) and ends with a vicinal disulfide bond (c20 – c21) at the tip of the finger. Interestingly, cysteine mutations in the index finger did not overtly affect secretion, although a higher amount of oxidized oligomers was detected compared with the WT Wnt3a. Note that among all cysteine mutations, those within the index finger generated the highest amount of monomeric Wnt3a (Fig. 2*C*), probably reflecting quasinormal folding and secretion.

Activity of Wnt3a Single Cysteine Mutants—Next we examined the signaling activity of the Wnt3a single cysteine mutants. We co-transfected an expression vector for each Wnt3a WT or mutant with the Wnt/β-catenin-responsive SuperTopFlash (STF) luciferase reporter along with a control *Renilla* luciferase reporter. Ratios of STF/Renilla luciferase were normalized as a percentage of the Wnt3a WT activity (Fig. 2*D*). As expected, many of the Wnt3a mutants with impaired secretion exhibited no activity, and, except for those mutants in the index finger, the level of Wnt3a secretion generally correlated with residual activity. Reduction in signaling strength for the c3 mutant is consistent with previous reports for Wnt3a C77A (10, 19). Mutation at c4 or within the hairpin 1 region produced a similar reduction of activity. These data suggest that a portion of each mutant may be able to form the remaining disulfide bonds correctly even with one free cysteine and is in a monomeric (non-oxidized) form competent for receptor binding. Alternatively, the oxidized oligomer formation of these Wnt3a mutants may occur gradually after secretion, permitting signaling from the transient monomeric form before oxidized oligomers accumulate. Consistent with either of these possibilities, the areas surrounding cysteines c3– c8 neither interact with the FZD CRD in the Xwnt8 co-crystal nor overlap with the predicted or experimentally mapped LRP6 binding regions (18, 20, 21). In the index finger, mutation at either of the more proximal cysteines (c18 or c23) partially reduced activity, whereas the more distal pair (c19 and c22) displayed a severe reduction of activity (Fig. 2*D*). Importantly, mutation of either vicinal c20 or c21 ablated the activity despite the relative high or quasinormal levels of secreted monomeric Wnt3a (Fig. 2*D*). Our results are fully consistent with the Xwnt8-FZD8 CRD co-crystal structure in which c20 and c21 at the tip of the index finger directly interact with the FZD8 CRD (site 2) (18). Although neither the proximal (c18 – c23) nor distal (c19 – c22) cysteines directly contact the FZD8 CRD, these two disulfide bonds may perform moderate and significant roles, respectively, in holding the index finger conformation for FZD binding.

We note that our co-transfection condition potentially reflected the combination of autocrine and paracrine Wnt3a signaling. To confirm the paracrine effects of the Wnt3a mutants, we collected CM and applied it to responsive cells transfected with the luciferase reporter. The paracrine activity

TABLE 1

Summary of secretion and activity of Wnt3a cysteine mutants

Tabulated are the Wnt3a cysteine position (and the corresponding Xwnt8 cysteine position), protein levels in CM (under reducing and non-reducing conditions), and activity in the STF luciferase assays (performed by either cotransfection of the STF plasmid with the Wnt3a expression vector or by stimulation of the STF reporter-transfected cells with the Wnt3a CM collected for each mutant. Secretion or activity of the WT Wnt3a is set at 100%, and the normalized average values are shown with S.D.

				Secretion		Activity	
	Xwnt8	Wnt3a	Cys to Ala Mutant	Total WT= 100	Monomer WT= 100	Cotransfection WT= 100	CM treatment WT= 100±3
amino	x	42	c1	43 ±11	6 ±8	1 ±0	1 ±2
	x	56	c2	26 ±4	7 ±10	0 ±0	-3 ±4
	55	77	c3	62 ±2	10 ±11	34 ±2	18 ±2
	66	88	c4	69 ±8	21 ±20	67 ±3	59 ±3
hairpin 1	105	128	c5	59 ±6	19 ±21	23 ±1	24 ±1
	113	136	c6	70 ±14	24 ±12	55 ±7	26 ±2
	115	138	c7	67 ±14	35 ±22	52 ±8	32 ±4
	133	155	c8	69 ±24	39 ±28	54 ±2	44 ±6
hairpin 2 thumb	181	203	c9	13 ±9	4 ±5	2 ±0	14 ±3
	183	205	c10	17 ±15	5 ±6	0 ±0	10 ±3
	190	212	c11	25 ±9	10 ±7	1 ±0	-3 ±4
	195	217	c12	6 ±0	1 ±1	1 ±0	0 ±2
cysteine knot	260	281	c13	22 ±2	1 ±1	0 ±0	0 ±3
	276	297	c14	15 ±7	0 ±0	0 ±0	-3 ±4
	291	307	c15	42 ±5	6 ±6	0 ±0	3 ±2
	295	311	c16	10 ±1	0 ±0	0 ±0	5 ±2
	298	312	c17	15 ±1	1 ±1	0 ±0	3 ±2
hairpin 3 index finger	313	327	c18	61 ±11	33 ±14	67 ±8	37 ±7
	315	329	c19	79 ±19	22 ±9	5 ±0	5 ±2
	320	334	c20	89 ±27	29 ±5	0 ±0	5 ±3
	321	335	c21	111 ±28	34 ±2	0 ±0	6 ±4
	325	339	c22	86 ±31	31 ±6	15 ±1	24 ±3
	328	342	c23	95 ±41	32 ±11	58 ±2	26 ±3
	337	351	c24	32 ±13	1 ±1	0 ±0	0 ±3
Wnt3a double cysteine mutants			c1-c2	106 ±29	30 ±7	64 ±5	35 ±9
			c1-c3	86 ±36	3 ±1	0 ±0	-3 ±5
			c1-c4	11 ±11	0 ±0	0 ±0	2 ±2
			c2-c3	15 ±16	0 ±1	0 ±0	5 ±1
			c2-c4	6 ±6	0 ±0	0 ±0	4 ±1
			c3-c4	97 ±6	32 ±24	94 ±6	44 ±4
			c13-c17	62 ±20	4 ±1	0 ±0	1 ±3
			c14-c15	31 ±13	1 ±0	0 ±0	0 ±3
			c16-c24	5 ±6	0 ±0	0 ±0	-2 ±4
			c20-c21	83 ±30	88 ±11	0 ±0	-1 ±3

results from the CM were comparable and followed the same trend as those from the co-transfection experiment (Table 1).

A Disulfide Bond between Wnt3a c1 and c2—The amino c1 and c2 cysteines are not present in Xwnt8 but are present in most other Wnts, including Wnt3a (Fig. 1), and their integrity is essential for Wnt3a secretion and activity (Fig. 2, *C* and *D*). It seems likely that c1 and c2 form an additional disulfide bond characteristic to these Wnts. The severe reduction in secretion and loss of activity of the amino c1 or c2 mutant prompted us to make paired cysteine mutations to potentially rescue secretion and activity. We generated a series of six cysteine double mutants to test all of the possible disulfide bond pairings within the amino region. Consistent with the c3-c4 pairing in the Xwnt8 structure, the Wnt3a c3-c4 double mutant increased monomeric protein levels and activated the STF reporter similarly to WT Wnt3a (Fig. 3, *A* and *B*). The Wnt3a c1-c2 and c1-c3 double mutants were secreted; however, only the c1-c2 double mutant produced a significant amount of monomeric

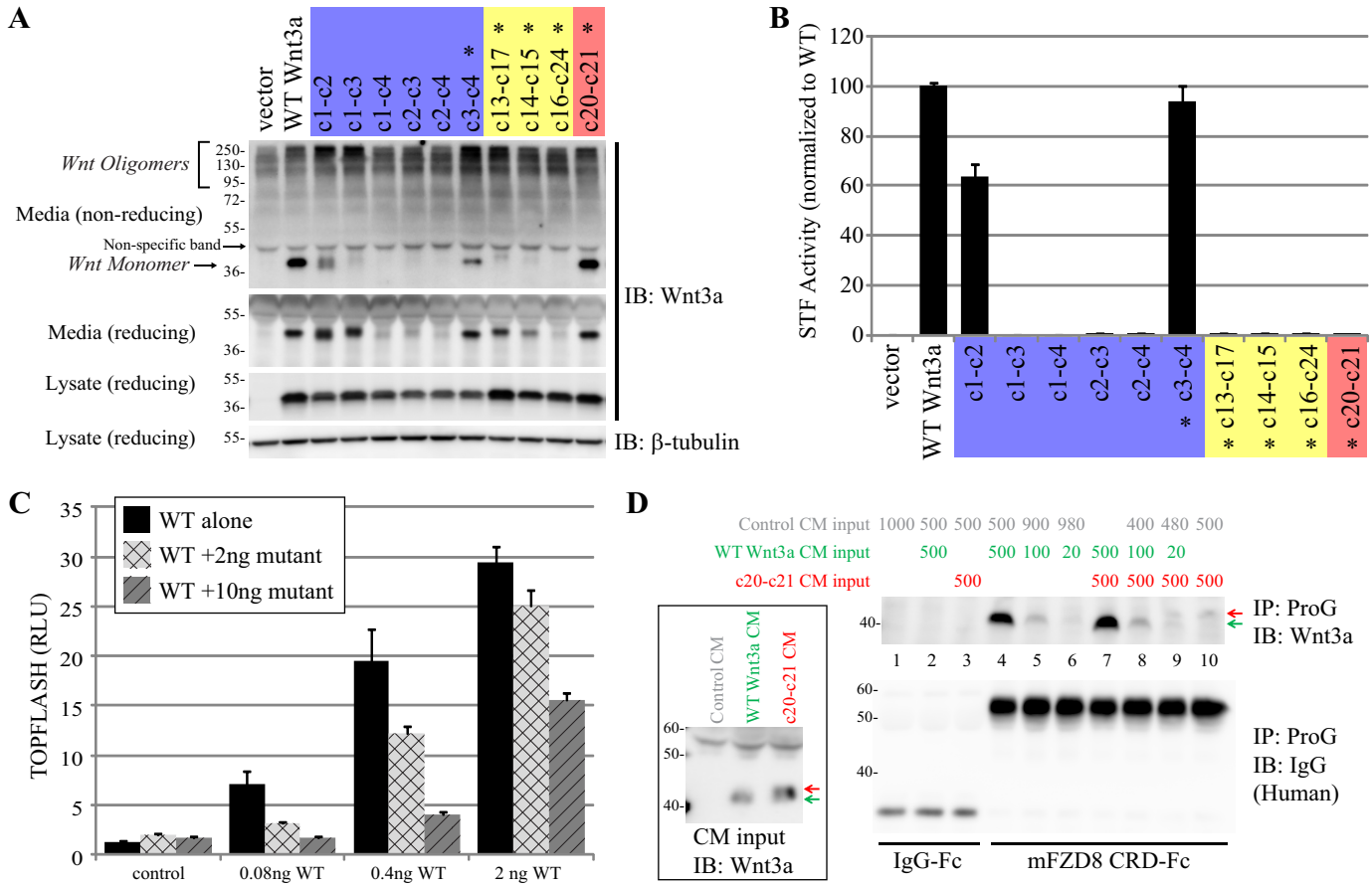

FIGURE 3. **Characterization of Wnt3a double cysteine mutants.** *A*, expression of Wnt3a double cysteine mutants in the whole cell lysate and CM using reducing and non-reducing conditions. *Asterisks* indicate positions of Xwnt8 resolved disulfide bonds. Relative density of the Wnt3a protein is quantified in Table 1. *B*, activity of the Wnt3a double mutants by cotransfection with the Wnt-responsive STF reporter. *C*, assessing the dominant negative activity of the Wnt3a c20-c21 mutant through varied dosages of WT and mutant expression constructs as indicated. *D*, co-immunoprecipitation of the WT Wnt3a or Wnt3a c20-c21 mutants with mFZD8 CRD-Fc. Input CM for the WT Wnt3a and the Wnt3a c20-c21 mutant is shown in the *inset*. Note that the c20-c21 mutant (*red arrow*) exhibits a slightly slower mobility than the WT Wnt3a (*green arrow*). *Error bars*, S.D. *IB*, immunoblot; *RLU*, relative luciferase units.

Wnt3a (Fig. 3*A*) and markedly restored the signaling activity (Fig. 3*B*). The remaining combinations of paired cysteine mutants were poorly secreted. Collectively, these data strongly support the notion of a c1-c2 disulfide bond that is critical for Wnt3a secretion.

Paired Cysteine Mutations in the Cysteine Knot Region—Single cysteine mutations within the cysteine knot region resulted in Wnt3a proteins with defective secretion, except for the c15 mutant that exhibited a low level of secretion of mostly oxidized oligomers (comparing detection under reducing and non-reducing conditions) (Fig. 2*C*). Because this region does not directly interact with FZD, we attempted to rescue the secretion and signaling defects using paired cysteine mutations. The c13-c17 and c14-c15 double mutants were secreted into the medium more efficiently; however, they were not monomeric and were mostly oxidized oligomers (Fig. 3*A*). The c16-c24 double mutant was present in the cell lysate but was barely detectable in the medium, indicating that this disulfide bond is essential for Wnt3a secretion. In parallel, signaling activity was not restored for any of the double cysteine mutants in the cysteine knot region (Fig. 3*B*). Therefore, in contrast to the amino-terminal region, where paired cysteine mutations of the respective disulfide bonds restore Wnt3a secretion and activity, ablation of any of the three disulfide bonds in the cysteine knot region inactivates the Wnt3a protein. Activity data from single and double cysteine mutants are summarized in Table 1.

The Wnt3a c20-c21 Double Mutant and Its Dominant Negative Activity—Of the single cysteine mutants of the index finger, the c20 or c21 mutant displayed the lowest or no signaling activity despite the presence of significant amounts of secreted monomeric Wnt3a (Fig. 2*C*). This is consistent with the critical role of the index finger in FZD binding (site 2) (18). Because the unpaired cysteine resulted in intermolecular oxidized oligomers (Fig. 2*C*), we generated the Wnt3a c20-c21 double mutant, which interestingly was secreted into the medium and remained monomeric to an extent comparable with the WT Wnt3a (Fig. 3*A*). However, this soluble Wnt3a c20-c21 mutant was inactive in the Wnt-responsive reporter assay (Fig. 3*B*). Furthermore, this mutant appeared to exhibit the dominant negative property, because it inhibited the WT Wnt3a signaling in a dosage-dependent manner in co-transfection assays (Fig. 3*C*).

The inactivity of the Wnt3a c20-c21 mutant probably reflects the essential contact made by these paired cysteines with FZD at site 2, which together with site 1 (formed by the palmitoleic acid and the thumb region with FZD) constitute the WNT-FZD

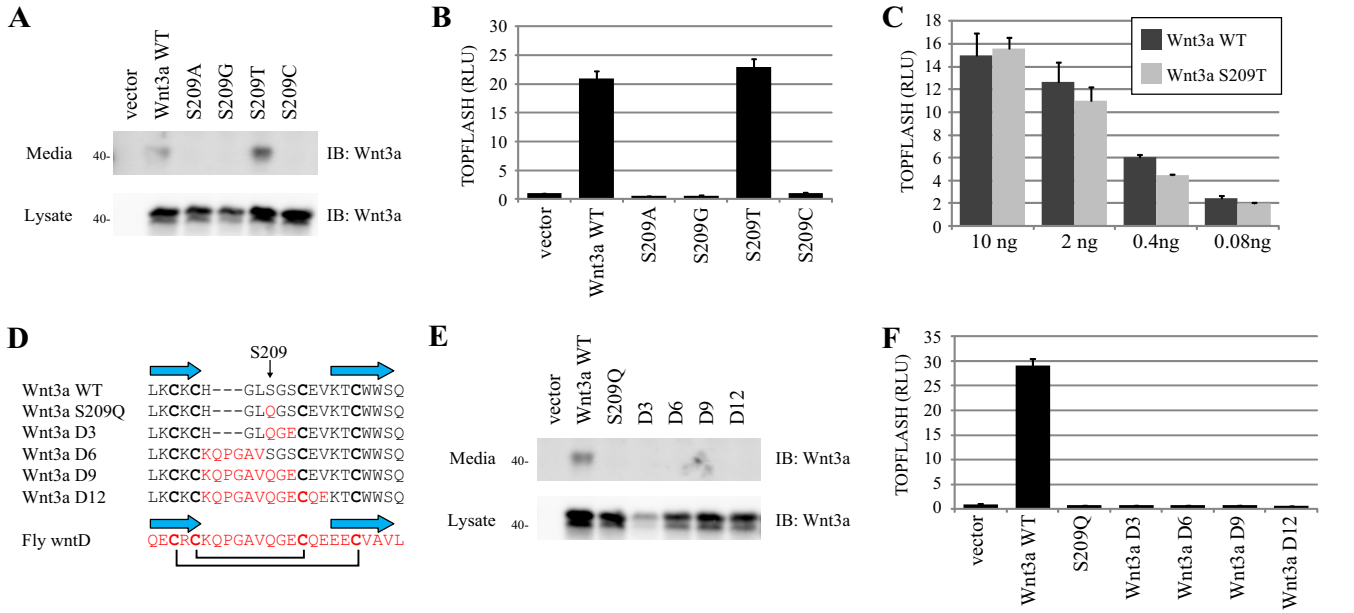

FIGURE 4. **The conserved Wnt serine residue for palmitoleic acid adduction can be functionally substituted by threonine but not other residues tested.** *A*, Wnt3a Ser-209 mutant expression (50 ng/well) in total cell lysate and in CM. *B*, the WNT-responsive STF luciferase reporter showing the activity of the WT Wnt3a and the active Wnt3a S209T substitution but the inactivity of S209A, S209G, or S209C substitution. *C*, similar levels of activity of the WT Wnt3a and Wnt3a S209T at multiple doses. *D*, Wnt3a mutants harboring substitutions of a portion of the thumb/hairpin 2 from *Drosophila* WntD (in *red*). Annotated β sheets above Wnt3a are modeled from the Xwnt8 structure, whereas those above WntD are from the WntD structure. The c9–c12 and c10–c11 disulfide bonds are indicated. *E*, protein expression levels of Wnt3a/WntD chimera mutants from transfected cells (at 50 ng/well of the expression vector) in total cell lysates and in CM. *F*, the WNT-responsive STF luciferase reporter showing the activity of the WT Wnt3a and the inactivity of each Wnt3a/WntD chimera mutant, including S209Q. *Error bars*, S.D. *IB*, immunoblot; *RLU*, relative luciferase units.

bipartite binding interface (18). Although the c20-c21 mutant results in a defective index finger tip at site 2, it probably retains the intact thumb region that permits secretion and engagement to FZD at site 1. To directly test the loss of FZD binding by the c20-c21 mutant, we performed a co-immunoprecipitation using a secreted form of the mouse FZD8 CRD tagged with IgG-Fc (mFZD8 CRD-Fc). Taking advantage of a slight migration difference between the WT Wnt3a and the c20-c21 mutant, we analyzed mFZD8 binding to the WT Wnt3a alone or in the presence of the c20-c21 mutant (Fig. 3*D*). As reported previously, WT Wnt3a bound to the mFZD8 CRD (19) in a dose-dependent manner, with higher input levels of Wnt3a resulting in higher amounts co-immunoprecipitated by mFZD8 CRD-Fc (Fig. 3*D*, *lanes 4–6*). However, the highest input level of the c20-c21 mutant only resulted in a small amount of immunoprecipitated mutant Wnt3a proteins (Fig. 3*D*, *lane 10*), confirming that the index finger mutant was severely defective for FZD binding. There is a roughly 25-fold reduction of FZD binding because the WT Wnt3a at a 20-μl input volume and the c20-c21 mutant at 500 μl yielded similar levels of the co-immunoprecipitation amount by mFZD8 CRD-Fc (Fig. 3*D*, *lanes 6* and *10*). The c20-c21 mutant did not appear to competitively inhibit FZD binding by WT Wnt3a, whose dose-dependent co-immunoprecipitation by mFZD8 CRD was comparable with or without the presence of the c20-c21 mutant at the maximal input level (500 μl) (Fig. 3*D*, *lanes 4–6 versus lanes 7–9*). These results suggest that the dominant negative activity of the c20-c21 mutant is probably contributed by its ability to bind to LRP6 via the intact Wnt palm region but its inability to bind to FZD, possibly in a manner similar to the action of Wnt inhibitors Dkk1 and sclerostin (26, 27). We note that the Wnt3a c20-c21 mutant shares some similarities with a dominant negative Xwnt8 mutant, which is truncated at the c13 position and thus lacks the carboxyl cysteine knot and index finger regions (28). Interestingly, a shorter Xwnt8 truncation lacking an additional 30 amino acids from the linker domain did not exhibit the effective dominant negative property (28), possibly due to truncating into the prospective LRP6 binding region. A similarly truncated and dominant negative Wnt3a mutant was recently reported (21).

Further Analysis of the Wnt3a Thumb Region—Having validated experimentally the key aspect (the vicinal disulfide bond at the tip) of the Wnt3a index finger, we further examined a cardinal feature of the thumb, the serine residue (Ser-209) that is palmitoleoylated. As reported previously, a S209A substitution abolished Wnt3a secretion and activity (9) (Fig. 4, *A* and *B*). Ser-209 substitution by glycine was similarly detrimental (Fig. 4, *A* and *B*). Interestingly, Ser-209 substitution by threonine was fully functional, as seen by the normal Wnt3a S209T secretion and signaling activity (Fig. 4, *A* and *B*). Analysis of CM under non-reducing condition revealed identical amounts of monomeric Wnt3a S209T compared with WT Wnt3a (data not shown), and Wnt3a S209T activity was equivalent to WT Wnt3a at all tested doses (Fig. 4*C*). This result was somewhat surprising, because this lipid-modified serine is invariant in vertebrate (and almost all invertebrate) Wnt proteins. One noticeable exception is a predicted Wnt from the primitive sponge *Oscarella* (OsWnt2), which has a threonine at this position (20, 29). This result implies that the Porcupine acyl transferase and the Wntless transporter can effectively use either serine or threonine at the thumb tip for lipid modification and transport recognition, respectively, and that FZD can fully recognize a

palmitoleoylate adducted to a threonine. On the other hand, although three predicted Wnt proteins from sponge *Oscarella* (OsWnt1) and cnidaria *Nematostella* (NvWnt5 and NvWnt10) contain a cysteine instead of a serine at the thumb tip position (30), we found that Wnt3a S209C was neither secreted nor active (Fig. 4, *A* and *B*). It remains possible that the ancestral Porcupine acylase in these primitive species specify for dual oxy- and thio-acylation abilities.

Drosophila WntD (Wnt inhibitor of Dorsal) is an unusual Wnt protein in that it harbors a glutamine instead of a serine at the thumb tip (31, 32). Unlike all of the Wnt proteins that have been examined thus far, WntD is secreted efficiently independent of Porcupine and Wntless functions (33) despite the fact that it has a similar structural fold as Xwnt8 (21). Locations of the β sheets and disulfide bonds in hairpin 2 in the WntD thumb are identical to those in Xwnt8, although WntD contains three additional amino acids in the thumb (Fig. 4*D*). In an attempt to obtain a secreted Wnt3a that is not lipidated and thus soluble aqueously, we generated a series of Wnt3a mutants that have the thumb tip region replaced by that of WntD. However, none of these Wnt3a mutants were secreted or displayed signaling activity (Fig. 4, *D–F*). Therefore, Wnt3a S209Q mutation or replacement of the thumb tip with portions of WntD did not seem to confer Porcupine/Wntless-independent secretion.

Active V5-tagged WNT Proteins—The Open Source *Wnt* Project aims to provide a full collection of all 19 human *WNT* cDNAs in versatile cloning and expression vectors for the research community (22). Each *WNT* cDNA was cloned into a gateway-compatible plasmid backbone either using the endogenous stop codon or in a "non-stop" format to enable fusion with an epitope tag or experimental protein. The *WNT* cDNA was then transferred into the pcDNA3.2/V5-DEST gateway destination expression vector for expression of untagged or carboxyl-terminal V5-tagged WNT proteins (22). These are highly desirable tools because antibodies for most WNT proteins are not available. Unfortunately, the published WNT-V5 version appears to produce only inactive proteins despite the detection of secreted WNT-V5 protein (22), leading to a discouraging impression that a carboxyl-terminal tag may be incompatible with WNT folding and activity. Upon careful inspection of these original WNT-V5 constructs, we noted the presence of an additional cysteine between WNT and the V5 tag introduced during the cloning process. Given the critical importance of the cysteine knot c16–c24 disulfide bond in Wnt3a, we suspect that this extra cysteine (an ectopic "c25"), which is unpaired, may be detrimental to WNT folding and responsible for the lack of activity. Therefore, we replaced the carboxyl-terminal gateway linker containing the extra cysteine with a short glycine linker in the WNT3A-V5 expression construct (see "Experimental Procedures"). We compared the expression of mouse Wnt3a (untagged, from Figs. 2 and 3); human WNT3A (untagged); the original V5-tagged version, referred to here as WNT3A-V5(+C linker); and the new modified V5-tagged version, referred to as WNT3A-V5a ("a" for active) (Fig. 5*A*). Untagged mouse Wnt3a and human WNT3A were expressed and secreted into the media at similar levels and migrate predominantly at the monomeric size under the non-reducing condition. In contrast, the inactive WNT3A-V5(+C linker) was absent in the monomeric fraction but present in the high molecular weight fraction of oxidized oligomers (Fig. 5*A*) (data not shown). The WNT3A-V5a protein in CM, on the other hand, resembled untagged Wnt3a and WNT3A and was primarily in the monomeric fraction under the non-reducing condition (Fig. 5*A*). Under the reducing condition, WNT3A-V5a appeared to be a doublet, due possibly to differential glycosylation (Fig. 5*A*).

Next we compared these two WNT-V5 expression constructs using the TOPFLASH assay. Whereas WNT3A-V5(+C linker) was inactive, as reported previously (22) (data not shown), WNT3A-V5a displayed significant activity (Fig. 5*B*). Compared with WNT3A, there was a slight reduction in activity for WNT3A-V5a, although this is not uncommon for epitope-tagged proteins. In co-transfection assays, WNT3A and WNT3-V5a demonstrated strong and comparable synergy with LRP6 (Fig. 5*C*). In addition, WNT3A and WNT3A-V5a induced similar levels of phosphorylation of Dishevelled (Fig. 5*D*), a downstream component common for both canonical and non-canonical Wnt signaling (34). Phosphorylation of Dishevelled correlates best with non-canonical Wnt signaling, which Wnt3a is also able to activate (1, 9, 22). WNT3A-V5a is therefore active for both canonical and non-canonical Wnt signaling.

Encouraged by these results, we modified the remaining 18 human WNT-V5(+C linker) expression constructs in a manner identical to what we had done for WNT3A-V5a. WNT protein expression and secretion were confirmed in total cell lysates and in CM, respectively (Fig. 5*E*). WNT-V5a proteins exhibited faster mobility than WNT-V5(+C linker) proteins, consistent with the deletion of 22 amino acids from the gateway linker region. Using the TOPFLASH assay in HEK293T cells, we compared the activity of untagged WNTs and WNT-V5a proteins. We observed strong activation of the reporter by WNT1, WNT2, WNT3, WNT3A, and WNT10B but not (or minimally) by the remaining WNTs (Fig. 5*B*), consistent with a previous report (22). Our results are also similar to those of a recent study that compared the canonical signaling activities of all 19 mouse Wnts in HEK293 cells (35). Thus, the majority of mouse and human WNTs are unable to activate canonical signaling in these cell lines, with the caveat that the FZD expression pattern may be a contributing factor (22). The corresponding WNT-V5a displayed a similar or identical trend but with somewhat diminished activity (Fig. 5*B*). We also cotransfected a small amount of an LRP6 expression vector to examine WNT-LRP6 synergistic effects. Again WNT-V5a proteins displayed synergy comparable with that of untagged WNTs (Fig. 5*C*). We also compared a subset of WNTs for non-canonical activity by monitoring Disheveled phosphorylation. Cells transfected with either untagged or WNT-V5a expression constructs for WNT4, WNT5A, and WNT11 showed comparable induction of Dishevelled phosphorylation (Fig. 5*D*). Collectively, our results suggest that the new WNT-V5a expression vectors produce V5-tagged and active WNT proteins.

DISCUSSION

The Wnt protein structure, seen in Xwnt8 in complex with FZD8 CRD, was described 30 years after the first *Wnt* gene was discovered (18). This structure reveals a number of unusual and

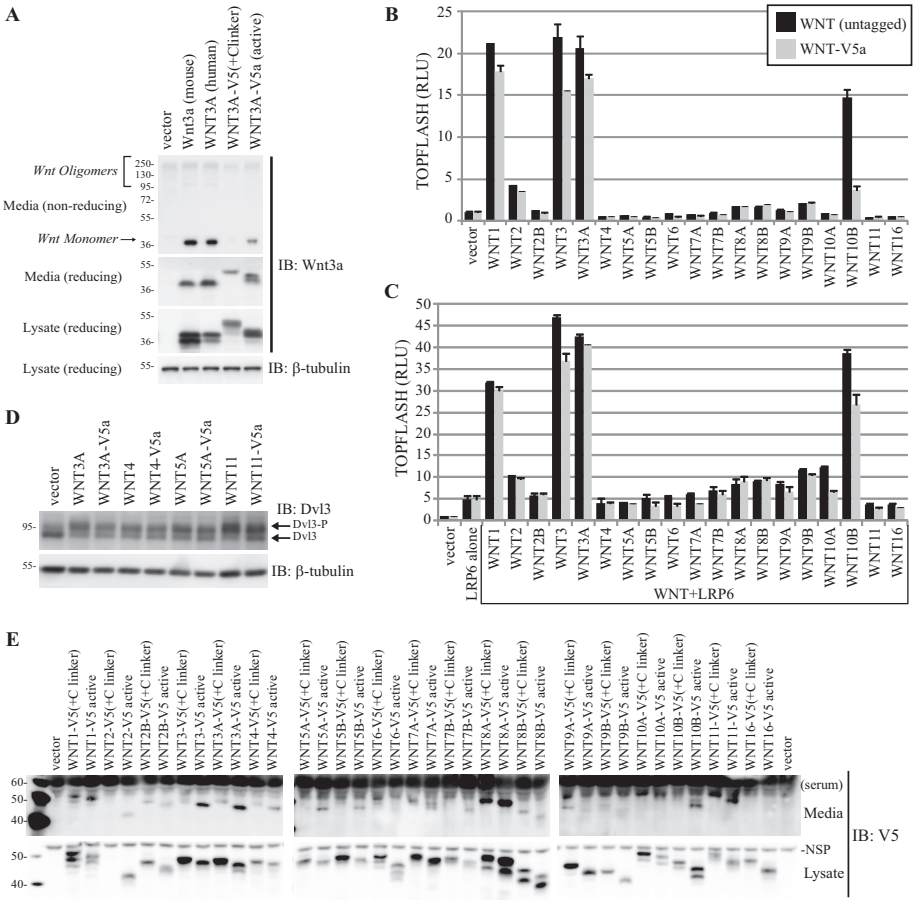

FIGURE 5. **Generation and characterization of the active V5 tagged WNT proteins.** *A*, comparison of untagged and two versions of V5-tagged WNT3A in non-reducing and reducing conditions. The previous V5(+C linker) and the new V5a constructs code for a WNT3A protein with a predicted addition of 4.4 and 1.9, kDa, respectively. *B*, the activity of untagged WNT proteins and new WNT-V5a assayed by the TOPFLASH reporter. 50 ng/well of each WNT expression vector was transfected. *C*, the activity of untagged WNT proteins and the new WNT-V5a in synergy with LRP6 assayed by the TOPFLASH reporter. 50 ng/well of each WNT expression vector plus 1 ng of LRP6 expression vector were co-transfected. *D*, the activity of untagged WNT proteins and the new WNT-V5a in non-canonical Wnt signaling measured by Dishevelled phosphorylation, which exhibits upward mobility shifts. *E*, comparison of WNT-V5 (+C linker) and WNT-V5a protein expression in whole cell lysates and CM under reducing conditions. The linker and the V5 tag for the original V5(+C linker) version (+CILKGGRADPAFLYVVDLLGPRFEGKPIPNPLLGLDSTRTG) was replaced by +GGGKPIPNPLLGLDSTRTG in the new WNT-V5a constructs. The V5(+C linker) and V5a add a predicted 4.4 and 1.9 kDa, respectively, to each WNT protein. Note that the WNT2-V5(+C linker) construct used in this experiment contains a frameshift mutation in the linker region that destroys the V5 tag. *Error bars*, S.D. *NSP*, nonspecific band in the lysate. *IB*, immunoblot; *RLU*, relative luciferase units.

unique features of the Wnt protein. These features include the bipartite binding of FZD by Wnt through the thumb, which is acylated at the tip, and the index finger, which harbors a vicinal disulfide bond at the tip, and a total of 11 pairs of disulfide bonds in the thumb and index finger and other regions across the entire Wnt molecule (18). This structure leads further to the proposal that Wnt proteins represent the fusion of an amino saposin-like domain (D1), which harbors the thumb region, and a carboxyl cytokine-like domain (D2), which contains the index finger region (20). The Wnt structure and the domain model provide critical insights into understanding the large family of Wnt proteins. However, many key features of the Wnt structure and model have not been experimentally examined. Through studies of Wnt secretion, FZD binding, and signaling activity, our systematic analysis of the cysteines and associated disulfide patterns and other key residues of the prototypic Wnt3a fully validate the prediction of the Wnt structure and domain arrangements. Our studies further lead to the generation of a set of expression vectors for Wnt research, including a full-length dominant-negative Wnt3a and a complete set of tagged and functionally active WNT proteins.

Wnt Disulfide Bonds and Subdomains Have Critical and Distinct Roles in Secretion and Activity—Most Wnt proteins, including Wnt3a, have 24 conserved cysteines, except for Wnt1 and Wnt8 (including Xwnt8), which have 22 cysteines and lack the two extra conserved cysteines at the amino terminus (Fig. 1). In Xwnt8, the 22 cysteines form 11 disulfide bonds in a pattern that is probably invariant among Wnt proteins, as reflected in the partial structure of a highly divergent *Drosophila* WntD (21). Our analyses of Wnt3a suggest a disulfide bond pattern fully consistent with that of Xwnt8 (and *Drosophila* WntD) and further suggest critical but distinct roles of these disulfide bonds in different Wnt subdomains.

We found that loss of each conserved cysteine in Wnt3a results in high molecular weight oxidized Wnt oligomers, which are formed through inter-Wnt disulfide bonding (Fig. 2*C*). Introduction of an ectopic cysteine in the early version of an epitope-tagged Wnt3a generated similar inactive oligomers (Fig. 5*A*). Some of these oxidized Wnt oligomers are present in CM, suggesting compatibility with secretion, whereas others are not secreted, a distinction that must depend on the location of the cysteine mutation and thus of the unpaired cysteine. We

reported previously that although the wild type Wnt3a is predominantly monomeric (non-oxidized) in CM, a significant amount of it exists as a high molecular weight oxidized oligomer species prior to secretion (19). Evidently, the initial Wnt3a disulfide bonds formed in the secretory pathway include erroneous intermolecular ones, implying that a crucial step during Wnt biogenesis is to shuffle Wnt disulfide bonds into the correct configuration prior to secretion, potentially via a disulfide isomerase. The existence of an unpaired cysteine in any Wnt3a cysteine mutants probably exacerbates (or impedes repairing) the various incorrect disulfide bonds, which differentially affect Wnt3a secretion.

In the saposin-like domain (D1), perturbation of disulfide bond formation in the hairpin 1 region has a rather mild effect on Wnt3a secretion and activity (Fig. 2). This probably reflects the fact that the conformation of the helical bundle (of four helices), which is devoid of disulfide bonds, is minimally affected, and that hairpin 1 may have some small effects on thumb/hairpin 2 conformation, given their proximity (Fig. 2). On the other hand, perturbation of disulfide bond formation in the thumb/hairpin 2 region abolishes Wnt3a secretion and activity (Fig. 2, *C* and *D*), suggesting a disruption of the thumb structure. This result is consistent with the fact that thumb is the site of Porcupine-dependent palmitoleoylation, which is required for binding to Wntless (for secretion) and FZD (site 1, for signaling).

In the cytokine-like domain (D2), perturbation of disulfide bond formation in the cysteine knot subregion is detrimental for Wnt3a secretion and activity (Fig. 2). This probably results from the fact that these three disulfide bonds are essential for the configuration of the entire cytokine-like domain, including holding in place the index finger structure through the very carboxyl terminus of the Wnt protein (Fig. 2). On the other hand, perturbation of disulfide bond formation in the index finger hairpin 3 does not affect Wnt3a secretion significantly but has small, medium, or detrimental effects on Wnt3a activity, respectively (Fig. 2). The vicinal disulfide bond at the very tip directly contacts FZD (site 2) in the Xwnt8 structure, accounting for its absolute requirement for Wnt3a activity. The two other disulfide bonds exhibit diminishing importance according to their distances to the vicinal one, probably reflecting their relative importance in holding the hairpin 3 structure and thus positioning the tip of the index finger.

In the Wnt3a amino terminus, a c3-c4 double mutant restores activity to almost that of the wild type Wnt3a (Fig. 3), suggesting further that c3 (Cys-77) is unlikely to be palmitoylated but rather forms a disulfide bond with c4 as seen in Xwnt8 and WntD (18, 21). This notion is consistent with other recent experimental evidence (15, 19). Surprisingly, mutation of the amino c1 or c2 position, neither of which exists in Xwnt8, abolishes Wnt3a secretion and activity (Fig. 2). It is likely that c1 and c2 form a disulfide bond, given that a c1-c2 double mutant restores significant Wnt3a secretion and activity (Fig. 3). These results suggest that the Wnt amino terminus, which is conserved among paralogues but is not conserved among the Wnt family (Fig. 1), has a pivotal role in Wnt biogenesis/secretion. We previously reported that TIKI proteases inactivate Wnt proteins, including Wnt3a via an amino-terminal cleavage (19). It is worth noting that TIKI cleavage of Wnt3a occurs amino-terminal to the c1 position (19) and therefore is unlikely to affect the c1–c2 disulfide bond formation. Indeed, TIKI-cleaved Wnt3a is secreted normally but forms inactive oxidized oligomers (19), in contrast to the c1 or c2 mutant that is barely secreted (Fig. 2). Thus, the Wnt amino terminus has distinct and essential roles in both Wnt secretion and activity. We note that TIKI also inactivates Xwnt8 via cleaving its amino terminus (19), which lacks both c1 and c2.

The Wnt3a c20-c21 Mutant Has Dominant Negative Activity—Paired mutations of Wnt3a c20-c21 at the tip of the index finger result in a dominant negative WNT protein, which is secreted as efficiently as the wild type Wnt3a but has drastically reduced binding to FZD (Fig. 3). To our knowledge, this is the first full-length Wnt mutant with dominant negative activity, a property that has only been shown so far for truncated Wnt mutants lacking the entire cytokine-like domain (21, 28). This result highlights the critical role of the vicinal c20–c21 disulfide bond of the index finger in FZD binding and provides a useful dominant negative reagent for Wnt studies. In this context, it is of interest to note that *Drosophila* WntD lacks the equivalent c20 and c21 cysteines, in addition to its lack of serine for acylation at the tip of the thumb region (21, 33). The absence of these cardinal features, which are invariable among almost all Wnt proteins, makes WntD unlikely to engage an FZD receptor. Indeed, WntD binds to neither Frizzled1 nor Frizzled2 in *Drosophila* (36).

Threonine Can Functionally Replace Serine as the Wnt Palmitoleoylation Site—We found that a Wnt3a S209T mutant was capable of secretion and signaling comparable with those of WT Wnt3a (Fig. 4). This is consistent with the predicted *O*-acyltransferase activity of the Porcupine enzyme and also suggests that Wntless and FZD engage Wnt3a S209T and the WT Wnt3a equivalently. Nearly all Wnt proteins contain serine at the palmitoleoylation site, and only one ancient Wnt protein from the sponge *Oscarella* (OsWnt2) contained a threonine at this position. It is unknown whether palmitoleoylation at the serine residue imparts unique advantages that warrant its conservation among Wnt proteins and whether threonine replacement of serine at the palmitoleoylation site of other Wnt proteins is tolerated.

During the revision of this manuscript, a similar result was reported, that a Wnt3a S209T substitution was functionally active and was lipidated identically as the WT Wnt3a using an ^{125}I-palmitoleate analog (37). Also similar to our findings, a Wnt3a S209C substitution resulted in an inactive Wnt3a (37). Curiously, a very small amount of lipidation was detected in the Wnt3a S209C, in contrast to Wnt3a S209A (37), suggesting that the mammalian Porcupine *O*-acyltransferase may inefficiently catalyze a thioester linkage between palmitoleate and the Wnt3a S209C mutant. This latent *S*-acyltransferase activity may be more pronounced in primitive metazoans, such as cnidaria and sponge, which possess Wnt proteins that contain a cysteine instead of a serine at the thumb tip position.

Significance of Wnt Cysteine Mutations in Development and Disease—Previous genetic and molecular studies have uncovered cysteine mutations in various Wnt proteins (Table 2). Probably the first WNT cysteine mutant to be characterized is

TABLE 2

Mutations of conserved cysteines in *Wg*, *WNT1*, *WNT5A*, *WNT10A*, and *WNT10B* in *Drosophila* development, functional assays, and human diseases, respectively

Cysteines are numbered using the c1–c24 nomenclature as described under "Results."

Cysteine position	Wg/WNT mutation	Disease or developmental phenotype
c1	*WNT5A* C69Y	Robinow syndrome (dominant), untested (52)
c2	*WNT5A* C83S	Robinow syndrome (dominant), hypomorphic (51)
c3	*WNT10A* C96R	Hypodontia/tooth agenesis (recessive), untested (44)
c4	*Wg* C104S	*Drosophila* mutant, partial activity (temperature-sensitive) (40)
c5	*WNT1* C143F	Osteogenesis imperfecta (recessive), untested (45)
c5	*WNT1* C143S	Site-directed mutagenesis, inactive (39)
c6	*WNT1* C151S	Site-directed mutagenesis, partial activity (temperature-sensitive) (39)
c8	*WNT5A* C182R	Robinow syndrome (dominant), hypomorphic (51)
c9	*WNT1* C219G	Early onset osteoporosis (dominant), inactive (48)
c11	*Wg* C242Y	Drosophila mutant, inactive (41)
c11	*WNT10B* C256Y	Obesity (dominant), inactive (42)
c12	*WNT10A* C276R	Oligodontia/tooth agenesis (recessive), untested (43)
c24	*WNT1* C369W	Site-directed mutagenesis, inactive (38, 39)

TABLE 3

Human WNT loss-of-function mutations resulting from an ectopic cysteine

Cysteines are numbered using the c1–c24 nomenclature as described under "Results."

The nearby cysteine and domain involved	WNT mutation	Human disease
c2 (+3), amino	*WNT5A* Y86C	Robinow syndrome (52)
c3 (+5), amino	*WNT4* R83C	Mullerian aplasia, hyperandrogenism (55)
c4 (+6), saposin-like, helix 1	*WNT10A* R113C	Oligodontia/tooth agenesis (44)
c7 (+12), saposin-like, hairpin1	*WNT10A* R171C	Oligodontia/tooth agenesis (44)
c8 (+7), saposin-like, helix 3	*WNT1* G177C	Osteogenesis imperfecta (46)
c8 (+9), saposin-like, helix 3	*WNT10A* R223C	Oligodontia/tooth agenesis (56)
c10 (+2), hairpin2/thumb	*WNT10A* G266C	Schopf-Schulz-Passarge syndrome (57)
c12 (+1), hairpin2/thumb	*WNT10A* W277C	Oligodontia/tooth agenesis (58)
c13 (−7), linker	*WNT10A* F339C	Oligodontia/tooth agenesis (43)
c13 (−1), cytokine-like, cysteine knot	*WNT1* F298C	Osteogenesis imperfecta (46, 47)
c14 (−6), cytokine-like, cysteine knot	*WNT10A* G356C	Oligodontia/tooth agenesis (59)
c14 (−2), cytokine-like, cysteine knot	*WNT7A* R292C	Fuhrmann syndrome (60)
c14 (−2), cytokine-like, cysteine knot	*WNT10A* R360C	Ectodermal dysplasia (61)
c17 (+2), cytokine-like, cysteine knot	*WNT10A* R379C	Ectodermal dysplasia (62)

the Wnt1 c24 mutant (*int*-1 C369W), which is inactive in the axis duplication assay in *Xenopus* embryos (38). The Wnt1 c5 mutant (C143S) is largely inactive, whereas the c6 mutant (C151S) is a hypomorphic temperature-sensitive allele in mouse mammary cell transformation assays (39). We observed a similar trend in our Wnt3a c5 and c6 mutants, with comparatively higher signaling activity for the Wnt3a c6 mutant than the Wnt3a c5 mutant (Fig. 2*D*). A *Drosophila* Wingless (*Wg*, the ortholog of *Wnt1*) mutant allele, wg^{IL114}, is a temperature-sensitive loss-of-function mutation at the c4 position (C104S), which is characterized by Wg secretion deficiency at non-permissive temperatures (40). On the other hand, wg^{NE6} is a null mutation at c11 (C242Y) in the thumb region (41). Similarly, at the c11 position, a heterozygous *WNT10B* mutation (C256Y) was identified in a genetic screen for obesity genes and was shown to be functionally inactive for Wnt signaling (42). *WNT10A* cysteine mutations (C96R, c3) and (C276R, c12) were also identified in patients with recessive tooth agenesis (43, 44). Although these *WNT10A* variants have not been functionally tested, the tooth agenesis phenotype was not as severe for the patient carrying the c3 mutation compared with other *WNT10A* loss-of-function alleles (44). These results parallel quite well those from our studies of Wnt3a (Fig. 2, *C* and *D*).

Loss-of-function missense and nonsense mutations of *WNT1* have been identified in patients with dominant early onset osteoporosis and recessive osteogenesis imperfecta, a human skeletal disorder (45–49). Two of the published *WNT1* mutations result in the loss of a conserved cysteine at c5 (C143F) near the saposin-like helical bundle and at c9 (C219G) in the thumb, respectively (45, 48). Our analyses of Wnt3a cysteine mutants suggest that c5 and c9 mutations would result in partial and complete inactivation, respectively. Indeed, the *WNT1* c9 (C219G) mutant shows a complete loss of function (48). Interestingly, a *WNT1* osteogenesis imperfecta truncation mutant (S295*) displays dominant negative properties in functional assays (48), consistent with the fact that the *WNT1* S295* truncation position is similar to that of the dominant negative Xwnt8 truncation (28).

Our studies of Wnt3a also appear to be useful for interpreting *WNT5A* mutations in Robinow syndrome, which was initially described in a family with dominantly segregating symptoms of short stature, hypertelorism, and mandibular hypoplasia (50). The causative mutation was later revealed to be at the c8 position of *WNT5A* (C182R), resulting in a partial loss of activity in non-canonical Wnt signaling (51). Loss-of-function *WNT5A* mutations in the amino c1 (C69Y) and c2 (C83S) have also been reported in patients with dominant Robinow syndrome (51, 52). Based on our results regarding the presence of a Wnt3a c1–c2 disulfide bond that is essential for secretion and activity, the *WNT5A* loss-of-function c1 or c2 mutation in Robinow syndrome may be fully explained. Therefore, although WNT5A acting through ROR1/2 receptors underlies its causation of Robinow syndrome, principles we gained from Wnt3a appear to be broadly applicable to other Wnt proteins, including those acting through non-canonical signaling.

In addition to these mutations at the conserved cysteine residues, 14 missense mutations that result in an ectopic cysteine have been identified in human patients with *WNT* loss-of-function phenotypes (Table 3). The gain of a cysteine in these WNT proteins appears to result in loss-of-function effects analogous to that by the ectopic c25 in WNT3A-V5 (+C linker) (Fig. 5). Overall data regarding sporadic cysteine mutations found or generated in different Wnt proteins in *Drosophila*, *Xenopus*, and human studies largely agree with our results derived from systematic analyses of Wnt3a. Therefore, our results should provide a useful guide for future investigation of diseases associated with *WNT* mutations.

An Expression Vector Set for Tagged Human WNT Proteins—Most WNT proteins terminate one or two residues after the c24 position, with the exception of WNT2/2B and WNT8A/8B (Fig. 1). The 20-amino acid residue region carboxyl-terminal to c24 is dispensable for Xwnt8 signaling (53). The presence of such a variable, and apparently non-essential, carboxyl-terminal extension in the WNT2 and WNT8 subfamilies implies that a carboxyl epitope tag may be tolerated in Wnt proteins. The previous version of WNT-V5 (+C linker) expression vectors appears to generate carboxyl V5-tagged WNT proteins that are inactive (22). Our analyses suggest that an extra cysteine (ectopic c25) introduced during cloning may be responsible for the inactivity, which correlates with the complete absence of monomeric WNT3A in CM (Fig. 5). Indeed, by deleting this ectopic cysteine (plus additional ectopic residues remaining from the cloning procedure), we have generated a new set of WNT-V5a expression vectors for all 19 human *WNT* genes. These vectors appear to produce V5-tagged WNT proteins that are functionally active in both canonical and non-canonical Wnt signaling assays (Fig. 5), showcasing a valuable set of tools for WNT studies. These vectors are now available at Addgene for distribution.

In addition to the carboxyl V5 tag, we have reported that an amino-terminal HA tag in Wnt3a (after the signal peptide cleavage) permits secretion and activity of HA-Wnt3a (19). In contrast, we found that a single amino-terminal FLAG tag in Wnt3a lowers the signaling activity considerably.[5] A reduction in activity is also noted for FLAG-WNT3A in a recent publication (54). We speculate that the highly acidic FLAG tag (DYKDDDDK) is less well tolerated in Wnt3a than the HA tag (YPYDVPDYA). Indeed, three tandem FLAG tags at the amino terminus, as expressed from the 3xFLAG-WNT vectors, render the tagged WNT proteins inactive (22).

In summary, our systematic analyses of conserved cysteine residues and resulting disulfide bonds in Wnt3a provide experimental validation for several key features observed in the Xwnt8 crystal structure, thus yielding important insights into Wnt protein domains, secretion, and activity. We also show that the critical and mostly invariable serine residue that is acylated in Wnt3a can be replaced by a threonine without any detectable effect on Wnt3a secretion or activity. In addition, our studies generate a set of expression vectors for producing tagged human WNT proteins that are functionally active and a novel dominant negative full-length Wnt protein. Finally, we emphasize that although our current and previous (19) studies indicate that the active Wnt3a protein is monomeric (non-oxidized) whereas inactive Wnt3a is oligomeric under the non-reducing electrophoresis condition, it remains possible that the active form of the Wnt3a protein in CM is a monomer or non-covalent oligomer.

[5] X. Zhang and X. He, unpublished results.

Acknowledgments—We thank members of the He laboratory for helpful comments.

REFERENCES

1. MacDonald, B. T., Tamai, K., and He, X. (2009) Wnt/β-catenin signaling: components, mechanisms, and diseases. *Dev. Cell* **17,** 9–26
2. Clevers, H., and Nusse, R. (2012) Wnt/β-catenin signaling and disease. *Cell* **149,** 1192–1205
3. Anastas, J. N., and Moon, R. T. (2013) WNT signalling pathways as therapeutic targets in cancer. *Nat. Rev. Cancer* **13,** 11–26
4. Willert, K., and Nusse, R. (2012) Wnt proteins. *Cold Spring Harb. Perspect. Biol.* **4,** a007864
5. Coudreuse, D., and Korswagen, H. C. (2007) The making of Wnt: new insights into Wnt maturation, sorting and secretion. *Development* **134,** 3–12
6. Holstein, T. W. (2012) The evolution of the Wnt pathway. *Cold Spring Harb. Perspect. Biol.* **4,** a007922
7. van Amerongen, R. (2012) Alternative Wnt pathways and receptors. *Cold Spring Harb. Perspect. Biol.* **4,** a007914
8. MacDonald, B. T., and He, X. (2012) Frizzled and LRP5/6 receptors for Wnt/β-catenin signaling. *Cold Spring Harb. Perspect. Biol.* **4,** a007880
9. Shibamoto, S., Higano, K., Takada, R., Ito, F., Takeichi, M., and Takada, S. (1998) Cytoskeletal reorganization by soluble Wnt-3a protein signalling. *Genes Cells* **3,** 659–670
10. Willert, K., Brown, J. D., Danenberg, E., Duncan, A. W., Weissman, I. L., Reya, T., Yates, J. R., 3rd, and Nusse, R. (2003) Wnt proteins are lipid-modified and can act as stem cell growth factors. *Nature* **423,** 448–452
11. Komekado, H., Yamamoto, H., Chiba, T., and Kikuchi, A. (2007) Glycosylation and palmitoylation of Wnt-3a are coupled to produce an active form of Wnt-3a. *Genes Cells* **12,** 521–534
12. Takada, R., Satomi, Y., Kurata, T., Ueno, N., Norioka, S., Kondoh, H., Takao, T., and Takada, S. (2006) Monounsaturated fatty acid modification of Wnt protein: its role in Wnt secretion. *Dev. Cell* **11,** 791–801
13. Rios-Esteves, J., and Resh, M. D. (2013) Stearoyl CoA desaturase is required to produce active, lipid-modified Wnt proteins. *Cell Rep.* **4,** 1072–1081
14. Kadowaki, T., Wilder, E., Klingensmith, J., Zachary, K., and Perrimon, N. (1996) The segment polarity gene porcupine encodes a putative multitransmembrane protein involved in Wingless processing. *Genes Dev.* **10,** 3116–3128
15. Gao, X., and Hannoush, R. N. (2014) Single-cell imaging of Wnt palmitoylation by the acyltransferase porcupine. *Nat. Chem. Biol.* **10,** 61–68
16. Coombs, G. S., Yu, J., Canning, C. A., Veltri, C. A., Covey, T. M., Cheong, J. K., Utomo, V., Banerjee, N., Zhang, Z. H., Jadulco, R. C., Concepcion, G. P., Bugni, T. S., Harper, M. K., Mihalek, I., Jones, C. M., Ireland, C. M., and Virshup, D. M. (2010) WLS-dependent secretion of WNT3A requires Ser^{209} acylation and vacuolar acidification. *J. Cell Sci.* **123,** 3357–3367
17. Cong, F., Schweizer, L., and Varmus, H. (2004) Wnt signals across the plasma membrane to activate the β-catenin pathway by forming oligomers containing its receptors, Frizzled and LRP. *Development* **131,** 5103–5115
18. Janda, C. Y., Waghray, D., Levin, A. M., Thomas, C., and Garcia, K. C. (2012) Structural basis of Wnt recognition by Frizzled. *Science* **337,** 59–64
19. Zhang, X., Abreu, J. G., Yokota, C., MacDonald, B. T., Singh, S., Coburn, K. L., Cheong, S. M., Zhang, M. M., Ye, Q. Z., Hang, H. C., Steen, H., and He, X. (2012) Tiki1 is required for head formation via Wnt cleavage-

oxidation and inactivation. *Cell* **149,** 1565–1577
20. Bazan, J. F., Janda, C. Y., and Garcia, K. C. (2012) Structural architecture and functional evolution of Wnts. *Dev. Cell* **23,** 227–232
21. Chu, M. L., Ahn, V. E., Choi, H. J., Daniels, D. L., Nusse, R., and Weis, W. I. (2013) Structural Studies of Wnts and identification of an LRP6 binding site. *Structure* **21,** 1235–1242
22. Najdi, R., Proffitt, K., Sprowl, S., Kaur, S., Yu, J., Covey, T. M., Virshup, D. M., and Waterman, M. L. (2012) A uniform human Wnt expression library reveals a shared secretory pathway and unique signaling activities. *Differentiation* **84,** 203–213
23. Chen, S., Bubeck, D., MacDonald, B. T., Liang, W. X., Mao, J. H., Malinauskas, T., Llorca, O., Aricescu, A. R., Siebold, C., He, X., and Jones, E. Y. (2011) Structural and functional studies of LRP6 ectodomain reveal a platform for Wnt signaling. *Dev. Cell* **21,** 848 – 861
24. MacDonald, B. T., Yokota, C., Tamai, K., Zeng, X., and He, X. (2008) Wnt signal amplification via activity, cooperativity, and regulation of multiple intracellular PPPSP motifs in the Wnt co-receptor LRP6. *J. Biol. Chem.* **283,** 16115–16123
25. Bruhn, H. (2005) A short guided tour through functional and structural features of saposin-like proteins. *Biochem. J.* **389,** 249 –257
26. Cruciat, C. M., and Niehrs, C. (2013) Secreted and transmembrane wnt inhibitors and activators. *Cold Spring Harb. Perspect. Biol.* **5,** a015081
27. Bourhis, E., Wang, W., Tam, C., Hwang, J., Zhang, Y., Spittler, D., Huang, O. W., Gong, Y., Estevez, A., Zilberleyb, I., Rouge, L., Chiu, C., Wu, Y., Costa, M., Hannoush, R. N., Franke, Y., and Cochran, A. G. (2011) Wnt antagonists bind through a short peptide to the first β-propeller domain of LRP5/6. *Structure* **19,** 1433–1442
28. Hoppler, S., Brown, J. D., and Moon, R. T. (1996) Expression of a dominant-negative Wnt blocks induction of MyoD in *Xenopus* embryos. *Genes Dev.* **10,** 2805–2817
29. Lapébie, P., Gazave, E., Ereskovsky, A., Derelle, R., Bézac, C., Renard, E., Houliston, E., and Borchiellini, C. (2009) WNT/β-catenin signalling and epithelial patterning in the homoscleromorph sponge *Oscarella*. *PLoS One* **4,** e5823
30. Kusserow, A., Pang, K., Sturm, C., Hrouda, M., Lentfer, J., Schmidt, H. A., Technau, U., von Haeseler, A., Hobmayer, B., Martindale, M. Q., and Holstein, T. W. (2005) Unexpected complexity of the Wnt gene family in a sea anemone. *Nature* **433,** 156 –160
31. Gordon, M. D., Dionne, M. S., Schneider, D. S., and Nusse, R. (2005) WntD is a feedback inhibitor of Dorsal/NF-κB in *Drosophila* development and immunity. *Nature* **437,** 746 –749
32. Ganguly, A., Jiang, J., and Ip, Y. T. (2005) Drosophila WntD is a target and an inhibitor of the Dorsal/Twist/Snail network in the gastrulating embryo. *Development* **132,** 3419 –3429
33. Ching, W., Hang, H. C., and Nusse, R. (2008) Lipid-independent secretion of a *Drosophila* Wnt protein. *J. Biol. Chem.* **283,** 17092–17098
34. Yanagawa, S., van Leeuwen, F., Wodarz, A., Klingensmith, J., and Nusse, R. (1995) The dishevelled protein is modified by wingless signaling in *Drosophila*. *Genes Dev.* **9,** 1087–1097
35. Yu, H., Ye, X., Guo, N., and Nathans, J. (2012) Frizzled 2 and frizzled 7 function redundantly in convergent extension and closure of the ventricular septum and palate: evidence for a network of interacting genes. *Development* **139,** 4383– 4394
36. Wu, C. H., and Nusse, R. (2002) Ligand receptor interactions in the Wnt signaling pathway in *Drosophila*. *J. Biol. Chem.* **277,** 41762– 41769
37. Rios-Esteves, J., Haugen, B., and Resh, M. D. (May 5, 2014) Identification of key residues and regions important for Porcupine-mediated Wnt acylation. *J. Biol. Chem.* M114.561209
38. McMahon, A. P., and Moon, R. T. (1989) Ectopic expression of the proto-oncogene int-1 in *Xenopus* embryos leads to duplication of the embryonic axis. *Cell* **58,** 1075–1084
39. Mason, J. O., Kitajewski, J., and Varmus, H. E. (1992) Mutational analysis of mouse Wnt-1 identifies two temperature-sensitive alleles and attributes of Wnt-1 protein essential for transformation of a mammary cell line. *Mol. Biol. Cell* **3,** 521–533
40. van den Heuvel, M., Harryman-Samos, C., Klingensmith, J., Perrimon, N., and Nusse, R. (1993) Mutations in the segment polarity genes wingless and porcupine impair secretion of the wingless protein. *EMBO J.* **12,** 5293–5302
41. Dierick, H. A., and Bejsovec, A. (1998) Functional analysis of Wingless reveals a link between intercellular ligand transport and dorsal-cell-specific signaling. *Development* **125,** 4729 – 4738
42. Christodoulides, C., Scarda, A., Granzotto, M., Milan, G., Dalla Nora, E., Keogh, J., De Pergola, G., Stirling, H., Pannacciulli, N., Sethi, J. K., Federspil, G., Vidal-Puig, A., Farooqi, I. S., O'Rahilly, S., and Vettor, R. (2006) WNT10B mutations in human obesity. *Diabetologia* **49,** 678 – 684
43. Song, S., Zhao, R., He, H., Zhang, J., Feng, H., and Lin, L. (2014) WNT10A variants are associated with non-syndromic tooth agenesis in the general population. *Hum. Genet.* **133,** 117–124
44. Mostowska, A., Biedziak, B., Zadurska, M., Dunin-Wilczynska, I., Lianeri, M., and Jagodzinski, P. P. (2013) Nucleotide variants of genes encoding components of the Wnt signalling pathway and the risk of non-syndromic tooth agenesis. *Clin. Genet.* **84,** 429 – 440
45. Fahiminiya, S., Majewski, J., Mort, J., Moffatt, P., Glorieux, F. H., and Rauch, F. (2013) Mutations in WNT1 are a cause of osteogenesis imperfecta. *J. Med. Genet.* **50,** 345–348
46. Keupp, K., Beleggia, F., Kayserili, H., Barnes, A. M., Steiner, M., Semler, O., Fischer, B., Yigit, G., Janda, C. Y., Becker, J., Breer, S., Altunoglu, U., Grünhagen, J., Krawitz, P., Hecht, J., Schinke, T., Makareeva, E., Lausch, E., Cankaya, T., Caparrós-Martín, J. A., Lapunzina, P., Temtamy, S., Aglan, M., Zabel, B., Eysel, P., Koerber, F., Leikin, S., Garcia, K. C., Netzer, C., Schönau, E., Ruiz-Perez, V. L., Mundlos, S., Amling, M., Kornak, U., Marini, J., and Wollnik, B. (2013) Mutations in WNT1 cause different forms of bone fragility. *Am. J. Hum. Genet.* **92,** 565–574
47. Pyott, S. M., Tran, T. T., Leistritz, D. F., Pepin, M. G., Mendelsohn, N. J., Temme, R. T., Fernandez, B. A., Elsayed, S. M., Elsobky, E., Verma, I., Nair, S., Turner, E. H., Smith, J. D., Jarvik, G. P., and Byers, P. H. (2013) WNT1 mutations in families affected by moderately severe and progressive recessive osteogenesis imperfecta. *Am. J. Hum. Genet.* **92,** 590 –597
48. Laine, C. M., Joeng, K. S., Campeau, P. M., Kiviranta, R., Tarkkonen, K., Grover, M., Lu, J. T., Pekkinen, M., Wessman, M., Heino, T. J., Nieminen-Pihala, V., Aronen, M., Laine, T., Kröger, H., Cole, W. G., Lehesjoki, A. E., Nevarez, L., Krakow, D., Curry, C. J., Cohn, D. H., Gibbs, R. A., Lee, B. H., and Mäkitie, O. (2013) WNT1 mutations in early-onset osteoporosis and osteogenesis imperfecta. *N. Engl. J. Med.* **368,** 1809 –1816
49. Faqeih, E., Shaheen, R., and Alkuraya, F. S. (2013) WNT1 mutation with recessive osteogenesis imperfecta and profound neurological phenotype. *J. Med. Genet.* **50,** 491– 492
50. Robinow, M., Silverman, F. N., and Smith, H. D. (1969) A newly recognized dwarfing syndrome. *Am. J. Dis. Child.* **117,** 645– 651
51. Person, A. D., Beiraghi, S., Sieben, C. M., Hermanson, S., Neumann, A. N., Robu, M. E., Schleiffarth, J. R., Billington, C. J., Jr., van Bokhoven, H., Hoogeboom, J. M., Mazzeu, J. F., Petryk, A., Schimmenti, L. A., Brunner, H. G., Ekker, S. C., and Lohr, J. L. (2010) WNT5A mutations in patients with autosomal dominant Robinow syndrome. *Dev. Dyn.* **239,** 327–337
52. Roifman, M., Marcelis, C., Paton, T., Marshall, C., Silver, R., Lohr, J., Yntema, H., Venselaar, H., Kayserili, H., van Bon, B., Seaward, G., Consortium, F. C., Brunner, H., and Chitayat, D. (2014) *De novo* WNT5A-associated autosomal dominant Robinow syndrome suggests specificity of genotype and phenotype. *Clin. Genet.* 10.1111/cge.12401
53. Hsieh, J. C., Rattner, A., Smallwood, P. M., and Nathans, J. (1999) Biochemical characterization of Wnt-frizzled interactions using a soluble, biologically active vertebrate Wnt protein. *Proc. Natl. Acad. Sci. U.S.A.* **96,** 3546 –3551
54. Green, J. L., Bauer, M., Yum, K. W., Li, Y. C., Cox, M. L., Willert, K., and Wahl, G. M. (2013) Use of a molecular genetic platform technology to produce human Wnt proteins reveals distinct local and distal signaling abilities. *PLoS One* **8,** e58395
55. Biason-Lauber, A., De Filippo, G., Konrad, D., Scarano, G., Nazzaro, A., and Schoenle, E. J. (2007) WNT4 deficiency: a clinical phenotype distinct from the classic Mayer-Rokitansky-Kuster-Hauser syndrome: a case report. *Hum. Reprod.* **22,** 224 –229
56. Arzoo, P. S., Klar, J., Bergendal, B., Norderyd, J., and Dahl, N. (2014) WNT10A mutations account for ¼ of population-based isolated oligodontia and show phenotypic correlations. *Am. J. Med. Genet. A* **164A,** 353–359
57. Castori, M., Castiglia, D., Brancati, F., Foglio, M., Heath, S., Floriddia, G.,

Madonna, S., Fischer, J., and Zambruno, G. (2011) Two families confirm Schopf-Schulz-Passarge syndrome as a discrete entity within the WNT10A phenotypic spectrum. *Clin. Genet.* **79,** 92–95

58. van den Boogaard, M. J., Créton, M., Bronkhorst, Y., van der Hout, A., Hennekam, E., Lindhout, D., Cune, M., and Ploos van Amstel, H. K. (2012) Mutations in WNT10A are present in more than half of isolated hypodontia cases. *J. Med. Genet.* **49,** 327–331
59. Kantaputra, P., Kaewgahya, M., Jotikasthira, D., and Kantaputra, W. (2014) Tricho-odonto-onycho-dermal dysplasia and WNT10A mutations. *Am. J. Med. Genet. A* **164A,** 1041–1048
60. Woods, C. G., Stricker, S., Seemann, P., Stern, R., Cox, J., Sherridan, E., Roberts, E., Springell, K., Scott, S., Karbani, G., Sharif, S. M., Toomes, C., Bond, J., Kumar, D., Al-Gazali, L., and Mundlos, S. (2006) Mutations in WNT7A cause a range of limb malformations, including Fuhrmann syndrome and Al-Awadi/Raas-Rothschild/Schinzel phocomelia syndrome. *Am. J. Hum. Genet.* **79,** 402–408
61. Cluzeau, C., Hadj-Rabia, S., Jambou, M., Mansour, S., Guigue, P., Masmoudi, S., Bal, E., Chassaing, N., Vincent, M. C., Viot, G., Clauss, F., Manière, M. C., Toupenay, S., Le Merrer, M., Lyonnet, S., Cormier-Daire, V., Amiel, J., Faivre, L., de Prost, Y., Munnich, A., Bonnefont, J. P., Bodemer, C., and Smahi, A. (2011) Only four genes (EDA1, EDAR, EDARADD, and WNT10A) account for 90% of hypohidrotic/anhidrotic ectodermal dysplasia cases. *Hum. Mutat.* **32,** 70–72
62. Plaisancie, J., Bailleul-Forestier, I., Gaston, V., Vaysse, F., Lacombe, D., Holder-Espinasse, M., Abramowicz, M., Coubes, C., Plessis, G., Faivre, L., Demeer, B., Vincent-Delorme, C., Dollfus, H., Sigaudy, S., Guillen-Navarro, E., Verloes, A., Jonveaux, P., Martin-Coignard, D., Colin, E., Bieth, E., Calvas, P., and Chassaing, N. (2013) Mutations in WNT10A are frequently involved in oligodontia associated with minor signs of ectodermal dysplasia. *Am. J. Med. Genet. A* **161A,** 671–678